ELSEVIER

Coordination Chemistry Reviews 227 (2002) 217–232

COORDINATION CHEMISTRY REVIEWS

www.elsevier.com/locate/ccr

Imido analogues of p-block oxoanions

Garreth M. Aspinall, May C. Copsey, Angela P. Leedham, Christopher A. Russell *

School of Chemistry, University of Bristol, Cantock's Close, Bristol BS8 1TS, UK

Received 3 October 2001; accepted 10 December 2001

Contents

Abstract

The synthesis of imido analogues of p-block oxoanions is a relatively new area of investigation. This review summarises synthetic routes towards such anions and gives an analysis of the structure and reactivity of complexes containing the following anions, $[B(NR)_3]^{3-}$; $[C(NR)_3]^{2-}$; $[Si(NR)_4]^{4-}$; $[P(NR)_4]^{3-}$; $[HP(NR)_3]^{2-}$; $[As(NR)_3]^{3-}$; $[Sb(NR)_3]^{3-}$; $[S(NR)_3]^{2-}$; $[Se(NR)_3]^{2-}$; $[Te(NR)_3]^{2-}$ and $[S(NR)_4]^{2-}$.

Keywords: Main group; Imido; Anions; Lithium

1. Introduction

The depth and varied nature of oxoanions of the p-block elements are huge, and the replacement of an oxygen centre by an isoelectronic imido group (=NR) is schematically a simple one and an idea that has enormous scope. However, whereas a relatively vast

* Corresponding author. Fax: +44-117-929-0509.
E-mail address: chris.russell@bristol.ac.uk (C.A. Russell).

0010-8545/02/$ - see front matter
PII: S0010-8545(02)00014-0

body of knowledge has been accumulated on the related imido transition metal species, in comparison the chemistry of main group imido complexes is relatively underdeveloped. Transition metal imido compounds of the general formula $[M(NR)_n(L)_m]$ (R, alkyl or aryl group; L, ligand) have been a focus of considerable activity in recent years, incorporating several fields of interest including unusual molecular and electronic structures, fundamental reactivity, and in industrially relevant areas such as alkene polymerization and metathesis catalysis. In these complexes, the imide is considered as either a $4e^-$ or a $6e^-$ ($\sigma+2\pi$) donor. As such, many of the complexes that have been synthesised can be viewed as derivatives of other isoelectronic species (Cp^-, $[RC{\equiv}CR]^{2-}$, O^{2-}, S^{2-}, N^{3-}). If the imido group is bent, the N centre is considered formally sp^2 hybridised, and the ligand will be formally a $4e^-$ ($\sigma+\pi$) donor system. However, if the imido group is linear, the ligand can be either a $4e^-$ ($\sigma+\pi$) donor or a $6e^-$ ($\sigma+2\pi$) donor depending on the orbital energy match between the ligand and the metal. Correspondingly, the variations in the orientation of the imido ligand in the corresponding p-block anions (that are bent to varying degrees) are a feature that we have sought to highlight in this review.

Recently this imbalance has started to be redressed with the discovery of a diverse series of anionic imido complexes of the main group elements. With the vast number of p-block oxoanions that are known (see Fig. 1 for a summary of the some of the more commonly encountered oxoanions), it is hoped that the corresponding imido anions summarised here will represent the tip of a very large iceberg. The aims of this review are to gather together the body of work that has been accumulated on imido analogues of the p-block oxoanions and to uncover their rich and varied chemistry.

Group 13	Group 14	Group 15	Group 16	Group 17	Group 18
$[BO_3]^{3-}$	$[CO_3]^{2-}$	$[NO_2]^-$			
		$[NO_3]^-$			
	$[SiO_4]^{4-}$	$[HPO_3]^{2-}$	$[SO_3]^{2-}$	$[ClO]^-$	
		$[PO_4]^{3-}$	$[SO_4]^{2-}$	$[ClO_2]^-$	
				$[ClO_3]^-$	
				$[ClO_4]^-$	
		$[AsO_3]^{3-}$	$[SeO_3]^{2-}$	$[BrO]^-$	
		$[AsO_4]^{3-}$	$[SeO_4]^{2-}$	$[BrO_3]^-$	
				$[BrO_4]^-$	
		$[SbO_3]^{3-}$	$[TeO_3]^{2-}$	$[IO]^-$	$[XeO_6]^{4-}$
				$[IO_3]^-$	
				$[IO_4]^-$	

Fig. 1. Selected oxoanions of the p-block elements.

Many of the advances in p-block imido anion chemistry that have occurred rely heavily on the corresponding developments in X-ray crystal mounting and data collection. Whereas this review will extensively use such data, it is not thought necessary or desirable to include detailed ORTEP pictures of the X-ray structures as the salient points are more easily discussed with the aid of simple line drawings. The interested reader who wishes to examine the structures in more detail is directed to the relevant primary texts.

The nomenclature that will be used when referring to the imido anions will not be the IUPAC names but simply the prefix imido to the corresponding oxoanion name, e.g. $[C(NR)_3]^{2-}$ will be referred to as imidocarbonate dianions rather than guanidinate dianions.

Following the submission of this text, a review by Brask and Chivers has appeared in *Angewandte Chemie* (International Edition in English, 2001, 40, 3960–3976) that covers a similar subject matter.

2. Synthetic approaches

The many and varied routes employed by transition element chemists to generate imido species dwarf those currently available to the main group chemist. An illustration of some of the methods employed in organoimido transition metal is shown below (taken from the extensive review by Wigley on organoimido complexes of the transition metals) [1].

- N–H bond cleavage of amines–amides

$$OsO_4 + {}^t\mathrm{BuNH_2} \rightarrow Os(N{}^t\mathrm{Bu})O_3$$

$$Cp^*_2TaCl(THF) + LiN(H)Ph \rightarrow Cp^*_2Ta(NPh)H \quad (1)$$

- Desilylation of silylamines–silylamides

$$CpNbCl_4 + (Me_3Si)_2NMe \rightarrow CpNb(NMe)Cl_2 \quad (2)$$

- Metathesis reactions using non-metallic NR sources

$$Re(OSiPh_3)O_3 + 3ArNCO \rightarrow Re(NAr)_3(OSiPh_3) + 3CO_2$$

$$Cl_4W(N{}^i\mathrm{Pr}) + CyN{=}C{=}NCy \rightarrow Cl_4W(NCy) + {}^i\mathrm{PrN{=}C{=}NCy}$$

$$Ta(CH{}^t\mathrm{Bu})Cl_3(THF)_2 + MeN{=}C(H)Ph \rightarrow Ta(NMe)Cl_3(THF)_2 \quad (3)$$

- Metathesis reactions using metallic NR sources

$$Cp^*Ta(NAr)Cl_2 + CpNb(NMe)Cl_2 \rightarrow Cp^*Ta(NMe)Cl_2 + CpNb(NAr)Cl_2 \quad (4)$$

- Oxidation of azides–azo compounds

$$MoCl_4(THF)_2 + N_3Ar \rightarrow Mo(NAr)Cl_4(THF)$$

$$TiCl_2(TMEDA)_2 + PhN{=}NPh \rightarrow Ti(NPh)Cl_2(TMEDA) \quad (5)$$

- From nitriles

$$MoCl_5 + ClC{\equiv}N + POCl_3 + Cl_2 \rightarrow Mo(NCCl_3)Cl_4(OPCl_3) \quad (6)$$

- From metal nitrides

$$[^nBu_4N][Ru(\equiv N)(CH_2SiMe_3)_4] + Me_3SiOTf \rightarrow Ru(=NSiMe_3)(CH_2SiMe_3)_4 \quad (7)$$

Main group chemists have developed alternative methods towards imido anions. Several different routes have been employed, the fruits of which will be discussed in the proceeding sections.

2.1. Mixed metallation using alkyllithium and p-block dimethylamido reagents

This method, extensively used by Wright et al. (see Sections 3.2.3 and 3.2.4), has been successful in the preparation of both imido and the related phosphinidene (RP^{2-}) anions of heavy Group 14 and 15 elements. The reactions employ dimethylamido p block metal reagents with primary amines and primary amido complexes of the alkali metals to give a range of imido compounds.

e.g.

$$E(NMe_2)_n + n[N(H)R]^- \rightarrow [E(NR)_n]^{n-} + nMe_2NH \quad (8)$$

The dimethylamido reagents {notably $Sn(NMe_2)_2$, $As(NMe_2)_3$, $Sb(NMe_2)_3$ and $Bi(NMe_2)_3$} act as potent bases towards a range of simple organic acids. The beauty of this approach lies in the flexibility it offers in defining the end product(s), with the stoichiometry employed in the reactions being of paramount importance. The main limitation of this particular method is the relatively small number of p-block element dimethylamido starting materials that engage in this type of reaction.

2.2. Nucleophilic addition to p-block imines

The groups of Chivers and Stalke have employed this approach which uses Group 16 imines as templates for nucleophilic addition reactions with the lithium salts of primary amines (see Sections 3.3.1 and 3.3.2). This generates imido anions that are analogues of a range of oxoanions.

e.g.

$$E(NR)_n + 2[N(H)R]^- \rightarrow [E(NR)_{n+1}]^{2-} + RNH_2 \quad (9)$$

This method provides a clean and efficient synthetic route towards imido anions. The main limitation on its potential general applicability is the relatively small number of main group imines that are known to exist.

2.3. Using dilithiates of primary amines

This method involves the preparation of dilithium salts of primary amines and subsequent reaction with p-block element halides to produce the corresponding imido anion.

$$RNH_2 + 2^nBuLi \rightarrow RNLi_2 \xrightarrow{ECl_n} E(NR)_n^{n-} \quad (10)$$

This represents a very direct approach to the imido anions but has a relatively restricted potential owing to the limited number of dilithium salts of primary amines, Li_2NR, that are known to exist. However, it has been successfully used by Chivers et al. (see Section 3.1.2) and further research into the parent dilithium imide salts may improve the general applicability of this synthetic route.

2.4. Sequential amination/metallation reactions

An alternative method involves amination of a p-block element halide followed by metallation using an alkyllithium base.

$$EX_n + nRNH_2 \xrightarrow{base} E\{N(H)R\}_n \xrightarrow{nR'Li} E(NR)_n^{n-} \quad (11)$$

It has been used by Russell et al. to prepare both Group 13 and Group 15 imido anions (see Sections 3, 3.2.1, 3.2.2 and 3.2.3). The method is both inexpensive and flexible and uses chemicals that are routinely available in many laboratories, but perhaps suffers from a lack of specificity in defining the end product(s).

3. Group 13

There is an extensive body of data concerning Group 13-nitrogen linkages and a relatively large number of Group 13-oxoanions. Despite this, imido analogues of these complexes are sparse. Recent studies by Chivers et al. into the reactions of alkyllithium reagents (RLi) with the trisaminoboranes, $B\{N(H)^tBu\}_3$ (3:1 equivalents), have shown the alkyllithium compounds acting as a base to remove two amide protons and as a nucleophile to substitute the third amide group to produce dilithio boraamindinate complexes $[Li_2\{RB(N^tBu\}_2\}]_x$ (**1**,

R = ^{n}Bu, $x = 2$; **2**, R = Me, $x = 3$) [2]. Our own studies into the related reaction of BCl_3 with 2-methoxyaniline (1:6 equivalents) in toluene, and subsequent metallation with ^{n}BuLi (three equivalents) showed the product to be $\{[Li_4B(NR)_3\cdot THF]^+[B^nBu_4]^-\cdot toluene\}_2$ (R = 2-methoxyphenyl, **3**) which contains the first example of a tris(imido) borate trianion—the imido analogue of the orthoborate trianion, $[BO_3]^{3-}$ [3] (Scheme 1).

$B\{N(H)^tBu\}_3 + 3R'Li \longrightarrow Li_2R'B\{N^tBu\}_2 + LiN(H)^tBu + 2R'H$

$B\{N(H)(NR)\}_3 + 3^nBuLi \longrightarrow \{[Li_4B(NR)_3\cdot THF]^+[B^nBu_4]^-toluene\}_2$

(R = 2-methoxyphenyl)

Scheme 1.

The reaction to form **3** is evidently not as straightforward as might be expected. It has been suggested that the initial amination of the BCl_3 with 2-methoxyaniline is probably incomplete, leaving free BCl_3 present at the metallation step [3]. Addition of ^{n}BuLi results in the production of LiB^nBu_4, that combines with the lithiation product of the proposed $B\{N(H)R\}_3$ intermediate to give a mixed anionic species with empirical formula $Li_4B(NR)_3B^nBu_4$ (i.e. the monomer of the observed product). Evidently, metallation of trisaminoboranes is heavily dependant on the nature of the amine used. The structure of **3** is illustrated in Fig. 2 with selected bond lengths and angles in Table 1.

The pseudo trigonal planar boron atom coordinates three imido nitrogen centers (sum of NBN angles 358.8°). The B–N distances of 1.440(4), 1.448(4) 1.492(4) Å are shorter than the commonly accepted literature values for single bonds (ca. 1.58 Å) but larger than for formal double bonds (ca. 1.40 Å) [4]. This is indicative of partial multiple bond character that would be expected as a consequence of lone pairs on the imido groups overlapping the vacant p orbital at the sp^2 boron centre. The fact that two B–N distances are considerably shorter than the third can be attributed to the fact that larger coordination numbers lead to longer bonds, as has been observed in related studies of tris(imido) silanes [5,6].

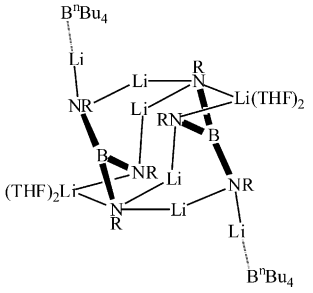

Fig. 2. Line drawing of the structure of $\{[Li_4B(NR)_3\cdot THF]^+[B^nBu_4]^-\cdot toluene\}_2$ (R = 2-methoxyphenyl, **3**).

Table 1
Selected structural data for the imidoborate trianion

$[B(NR)_3]^{3-}$	$\{[Li_4B(NR)_3\cdot THF]^+[B^nBu_4]^-$ (**3**)
Av. B···N (Å)	1.48
Av. N–B–N (°)	119.6
Li···N range (Å)	1.96–2.24
Av. B–N–C (°)	121.5
Reference	[3]

Similar imido p-block anions such as $[E(NR)_3]^{2-}$ (E = S, Se, Te, see Section 3.3) [7–9] where the pyramidal tris(imido) chalcogenide dianions allow the formation of cages of molecular C_{2h} symmetry, readily accommodate strong Li–N contacts in arrangements similar to those that are well known in lithium amide chemistry [10,11]. In contrast, the imposition of trigonal planar geometry at the boron centers in the central core of **1** does not easily facilitate comparable Li···N motifs. It has been suggested this inability to readily accommodate the bonding requirements of the lithium centers accounts, in part, for the difficulty in synthesising the direct imido analogue of the orthoborate trianion [3].

3.1. Group 14

Of the common Group 14 oxoanions, imido analogues of the carbonate dianion, the hydrogen carbonate monoanion and silicate tetraanion have been reported. Since the hydrogen carbonate monoanion is simply a protonated version of the carbonate dianion, its imido analogues will not be reviewed here, but the interested reader is directed towards a recent review in this journal by Bailey and Pace that gives a detailed description of the syntheses, structures and properties of the imido analogues of $[HCO_3]^-$ and $[CO_3]^{2-}$ [12]. This current review seeks to summarise the key points of the chemistry detailed in the previous article and to bring together the reports of other imido analogues of Group 14 oxoanions.

3.1.1. Imidocarbonate dianion

The first reported example of an imidocarbonate dianion was that of $[Fe(CO)_3\{\mu\text{-}C(NPh)_3\}Fe(CO)_3]$, from Farona et al. in 1971, but this was assigned only on the basis of spectroscopic analyses [13]. An X-ray crystallography study of a imidocarbonate ligand had to wait until 1995 when Bailey et al. reported the THF solvate of the dilithium salt, $[Li_2\{C(NPh)_3\}]$ (**4**), synthesised from the reaction of *N*,*N*′,*N*″-triphenylguanidine

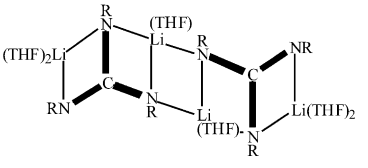

Fig. 3. Line drawing of the structure of $[(THF)_3Li_2\{C(NPh)_3\}]_2$ (**4**).

with two equivalents of ^{n}BuLi in THF [14]. It crystallises as a centrosymmetric dimer with a terminal lithium centre bridging two imido arms and being further coordinated by two THF ligands and a short contact to the *ipso–ortho* C···C bond of the phenyl ring. The second distinct lithium centre binds two separate $[C(NPh)_3]^{2-}$ units and is coordinated by a solitary THF molecule. This molecular geometry, illustrated in Fig. 3, resembles the ladder arrangements that are commonly encountered in lithium amide chemistry although chemically it is, of course, very different [10,11].

The central carbon atoms are planar {sum of angles around the central C is 360° although the individual NCN angles vary from 111.8(3) to 126.6(3)°} with all C–N bond distances equal within error at 1.36 Å, indicative of delocalised partial multiple bonding (cf. C–N 1.47 Å and C=N 1.30 Å) [15]. Low temperature ^{13}C-NMR studies show that all the phenyl groups are equivalent in solution. This has been attributed to either rapid rotation about the C–N bonds or the adoption of the symmetrical C_{2h} structure in solution.

A further dilithium salt of an imido carbonate, $[Li_2\{C(N^tBu)_3\}]$ (**5**) has recently been reported by Chivers et al. [16]. It was synthesised by addition of lithium amide to carbodiimides, as shown in Scheme 2.

Despite evident similarities in the chemical composition of **4** and **5**, the way in which they aggregate is very different, with **5** adopting a cage motif (see Fig. 4) whereas **4** forms a ladder type structure (as shown in Fig. 3). This has been ascribed to the solvation by THF in the former and the fact that it possesses Li···Ph contacts.

Complex **5** possesses $[C(N^tBu)_3]^{2-}$ dianion units which are essentially planar (sum of angles about central C is 358–359°, but in contrast to **4**, the NCN angles are ca. equal). The C–N bond lengths average 1.38 Å, slightly longer than in **4**, but consistent with a resonance hybrid with delocalised bonding. Solution ^{1}H- and ^{7}Li-NMR data for complex **5** show that the structure is highly fluxional (Table 2).

In addition, Henderson et al. reported imidocarbonate complexes of the d^6 metal ions, Ru(II), Os(II), Rh(III) and Ir(III), as well as the d^8 metal ion Pt(II), [17,18] from the Ag_2O mediated reactions of the platinum group metal complexes $[PtCl_2(COD)]$ (COD = 1,5-*cyclo*-octadiene), $[Cp^*MCl_2(PPh_3)]$, ($Cp^* = \eta^5$-C_5Me_5, M = Rh, Ir) and [(*p*-cymene)M′$Cl_2(PPh_3)$] (M′ = Ru, Os) with symmetrically trisubstiututed guanidines. Two of the products, the platinum complex, [Pt{C(NPh)$_3$}(COD)] (**6**) and the ruthenium complex [(*p*-cymene)Ru{C(NAc)$_3$}(PPh$_3$)]

$$^{t}BuN{=}C{=}N^{t}Bu + 2\,^{t}BuN(H)Li \longrightarrow [Li_2\{C(N^{t}Bu)_3\}]_2 + {}^{t}BuNH_2$$

Scheme 2.

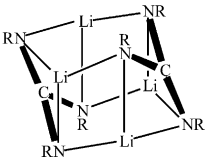

Fig. 4. Line drawing of the structure of $[Li_2\{C(N^tBu)_3\}]_2$ (**5**).

Table 2
Selected structural data for lithium salts of imidocarbonate dianions

$[C(NR)_3]^{2-}$	R = Ph (**4**)	R = ^{t}Bu (**5**)
Av. C···N (Å)	1.36	1.38
Av. N–C–N (°)	120.0	119.5
Li···N range (Å)	1.95–2.13	1.89–2.26
Av. C–N–C (°)	121.6	122.3
Reference	[14]	[16]

(**7**) were amenable to X-ray crystallographic investigations, although significant disorder and/or twinning in the latter prevents detailed analysis of the bond dimensions, but the bidentate binding mode of the imidocarbonate ligand is clear. In complex **6**, we have the first example of a mononuclear imidocarbonate complex, with the imidocarbonate ligand binding in a bidentate fashion with the charges localised on the donor centers (and hence formal double and single bond orders can be assigned to each of the C–N bonds). Once again, the imidocarbonate unit is planar (sum of angles around central C is 360°), and there are significant variations in each NCN angle which range from 103.3 (for the NCN angle incorporating the donating N centers) to 133.0°.

Complexes **6** and **7**, in addition to $[Cp^*M\{C(NR)_3\}(PPh_3)]$, (M = Rh, R = Ac, **8**; M = Rh, R = Ph, **9**; M = Ir, R = Ac, **10**) and [(*p*-cymene)Os{C(NAc)$_3$}(PPh$_3$)] (**11**) were studied by variable temperature NMR spectroscopy. This demonstrated the imidocarbonate moiety is fluxional at room temperature (r.t.), with the lone pair on the pendant nitrogen and the organic substituent on the same N center readily exchanging positions. It was shown this process could not be slowed sufficiently on the NMR timescale to resolve the two signals that would be expected from the solid-state structure.

The imidocarbonate ligand has also been identified in studies whereby tris(*iso*-propyl) guanidine has been deprotonated by the potent Group 15 base, tris(dimethylamido)antimony. The product [Sb{C(N^i-Pr)$_3$}{(^{i}PrN)$_2$C(NH^{i}Pr)}] (**12**) contains both the imidocarbonate ligand and the imido hydrogen carbonate ligand, with individual units of **12** linked in the solid state through N–H···N hydrogen bonding. However, the imidocarbonate and the imido hydrogen carbonate ligand cannot be readily distinguished owing to disorder in the crystal structure (the presence of the additional hydrogen atom can be observed in the ^{1}H-NMR spectra

and it is required by charge balancing arguments) and so this structure will not be discussed further.

Further investigation of the imidocarbonate ligands remains at an early stage. Nucleophilic addition of **4** to $Cd\{N(SiMe_3)_2\}_2$ gives the heterobimetallic complex $[\{(Me_3Si)_2N\}_2Cd\{C(NPh)_3\}Li_2\cdot 3THF]$ (13) [19]. The imidocarbonate moiety of **13** binds one of its arms to the cadmium centre and a further arm to a lithium centre in a monodentate fashion, whereas the other lithium centre bridges two arms of the imidocarbonate ligand. The reaction leaves the imidocarbonate unit essentially unchanged relative to the parent complex **4**, although there appears to be slight elongation of the C–N distance in the Cd coordinated arm {C–N 1.376(7) Å} relative to the other two {1.350(7) and 1.358(7) Å, respectively}.

Transmetallation reactions of **4** have also been investigated. Addition of **4** to a THF solution of Cp^*ZrCl_3 gives $[Cp^*\{C(NPh)_3\}ZrCl_2Li\cdot Et_2O\cdot THF]$ (**14**) [20]. Complex **14** shows modest ethylene polymerisation activity when mixed with MAO. Reaction of **14** with $LiNPh_2$ gives $[Cp^*\{C(NPh)_3\}ZrCl(NPh_2)Li(THF)_2]$ (**15**) which was amenable to an X-ray crystallographic study. Similarly, addition of **4** to $Cp^*TaMe_2Cl(OSO_3CF_3)$ gives $[Cp^*\{C(NPh)_3\}TaMe_2]$ (**16**) [20]. In both **15** and **16**, the imidocarbonate moiety binds in a bidentate fashion to the metal, having one short non-coordinating C–N arm and two relatively long coordinating C–N arms. The imidocarbonate unit in both structures contains a central planar C atom that possesses large deviations from regular trigonal planar geometry (Table 3).

It is noteworthy that in all of these examples the imidocarbonate ligand adopts a mono or bidentate binding mode, but never the η^3- mode commonly adopted by the isoelectronic trimethylenemethane (TMM) dianions, $[C(CH_2)_3]^{2-}$. This has been attributed to the fact that the TMM ligands undergo an umbrella distortion when binding to a metal, and this cannot be accommodated in the imidocarbonate ligands owing to stronger in-plane π-bonding in the case of the latter [12].

3.1.2. Imidosilicate tetraanion

A very direct route has been employed by Chivers et al. in the synthesis of the imidosilicate tetraanion. The dilithium salt of 1-aminonaphthalene was prepared and reacted with silicon tetrachloride in diethylether to give $[Li_4\{Si(Nnaphth)_4\cdot 4Et_2O]$ (**17**) [21] (Scheme 3).

$$4naphthNH_2 + 8^nBuLi + SiCl_4 \xrightarrow[-4LiCl]{-8^nBuH} [Li_4\{Si(Nnaphth)_4\}\cdot 4Et_2O]$$

Scheme 3.

Complex **17** was characterised by elemental analyses, IR and NMR (^1H, ^7Li and ^{29}Si) spectroscopy although it has not proved possible to obtain crystals suitable for X-ray crystallography. However, the reactivity of **17** towards both $^tBuNH_3Cl$ and MeO_3SCF_3 has been investigated and has been shown to produce $Si\{N(H)naph\}_4$ (**18**, the fully protonated derivative of **17**) and $Si\{N(Me)naph\}_4$ (**19**), respectively [21]. Attempts to deprotonate tetraaminosilanes related to **18** result in incomplete lithiation, with the only product that could be identified being the trilithium salt, $Li_3[Si\{N^iPr\}_3\{N(H)^iPr\}]\cdot THF$ (**20**). This incomplete lithiation has been attributed to steric crowding whereby the alignment of the *iso*-propyl substituents in the Li_6N_6 ladder sterically shield the remaining amido proton from nucleophilic attack by *n*-butyllithium [21].

3.2. Group 15

Imido analogues of the phosphate trianion, the phosphite dianion, the arsenate trianion and the antimonate trianion have been reported. In addition, Niecke et al. reported several structures that are imido analogues of kinetically unstable phosphorus oxoanions. This group described the planar tris(imino)metaphosphate anion, $[P(NR)_3]^-$ and the $[P(NR)_2]^-$ anion, isoelectronic with the kinetically unstable $[PO_3]^-$ and $[PO_2]^-$ anions, respectively, but more importantly related to the corresponding nitrate $[NO_3]^-$ and nitrite $[NO_2]^-$ anions [22,23]. These complexes will not be discussed any

Table 3
Selected structural data for non-lithium and heterobimetallic salts of imidocarbonate dianions

$[C(NR)_3]^{2-}$	$[Pt\{C(NPh)_3\}(COD)]$ (**6**)	$[\{(Me_3Si)_2N\}_2Cd\{C(NPh)_3\}Li_2\cdot 3THF]$ (**13**)	$[Cp^*\{C(NPh)_3\}ZrCl(NPh_2)Li(THF)_2]$ (**15**)	$[Cp^*\{C(NPh)_3\}TaMe_2]$ (**16**)
Av. C···N (Å)	1.37	1.36	1.36	1.36
Av. N–C–N (°)	120.0	120.0	120.0	120.0
Av. C–N–C (°)	124.0	122.1	121.9	122.7
Reference	[17]	[19]	[20]	[20]

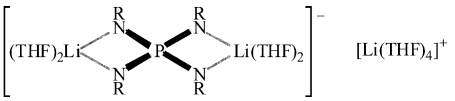

Fig. 5. Line drawing of the structure $[Li(THF)_4][(THF)_2Li(\mu\text{-}NR)_2P(\mu\text{-}NR)_2Li(THF)_2]$ (**21**).

Table 4
Selected structural data for the lithium salt of the imidophosphate trianion

$[P(NR)_4]^{3-}$	$[Li(THF)_4][(THF)_2Li(\mu\text{-}NR)_2P(\mu\text{-}NR)_2Li(THF)_2]$ (**21**)
Av. P···N (Å)	1.64
Av. N–P–N (°)	97.3 (bridged) and 115.9 (non-bridged)
Li···N (Å)	2.00
Av. P–N–C (°)	123.8
Reference	[24]

further as they are somewhat peripheral to the main theme of this review.

3.2.1. Imidophosphate trianions

The complex $[Li(THF)_4][(THF)_2Li(\mu\text{-}NR)_2P(\mu\text{-}NR)_2Li(THF)_2]$ (**21**) (R = naphthyl), which contains a $[P(NR)_4]^{3-}$ trianion which is isoelectronic with PO_4^{3-}, is produced in low but reproducible yield from the reaction of P_2I_4 with 1-aminonaphthalene (1:4 equivalents) in THF–NEt_3, followed by lithiation with ^{n}BuLi (four equivalents). A low-temperature X-ray crystallographic study of **21** (Fig. 5, Table 4) shows that it is an ion-separated complex containing a $[Li(THF)_4]^+$ cation and a $[(THF)_2Li(\mu\text{-}NR)_2P(\mu\text{-}NR)_2Li(THF)_2]^-$ anion [24].

The N atoms are arranged in a distorted-tetrahedral geometry about the central P atom, with Li cations bridging two pairs of N centers {N–Li 1.995(10) Å}. Each of these bridging Li cations has a distorted tetrahedral geometry with the coordination sphere being completed by two THF ligands. The P–N distances in the $[P(NR)_4]^{3-}$ anion {1.645(4) Å} are intermediate between those expected for a formal single bond (cf. 1.77 Å) and a formally double bonded P=N species (cf. 1.56–1.62 Å) [25]. Studies on related PN_4 anions and cations by Schnick et al. demonstrate that the observed bond lengths can be rationalised in terms of the formal bond order and the ionic contribution to the bond. Thus, in $[PN_4]^{7-}$, identified from solid-state studies of alkali metal phosphorus nitrides, the long (1.71 Å) bond length has been attributed to electrostatic repulsion between the highly negative N centers, [26] whereas, in the $[P(NH_2)_4]^+$ cation, the short (1.60 Å) bond length results from a high ionic contribution to the bond energy [27]. Evidently the bonding situation in **21** lies somewhere in between these two extremes. The bond angles around the central phosphorus atom show large distortions from perfect tetrahedral geometry (with two angles of 97.3(3), 113.1(3) and 118.7(3)°, respectively), presumably reflecting the strong binding of the N centers by the bridging Li atoms.

The mechanism by which **21** is formed is as yet unexplained. Studies on the reactivity of P_2I_4 are somewhat scarce, but nonetheless show a high degree of complexity [28]. It has been postulated that the most likely precursor is $[P\{N(H)naphth\}_4I]$, forming **21** readily by deprotonation [24].

3.2.2. Imidophosphite dianions

A similar reaction, that of PCl_3 with three equivalents of 2-methoxyaniline in THF–NEt_3, followed by metallation with ^{n}BuLi (two equivalents) yields a complex $[Li_2P(H)(NR)_3]_2$ (R = 2-methoxyphenyl, **22**), whose tris(imido) phosphonate anion is the imido analogue of the phosphite anion, $[HPO_3]^{2-}$ [29]. Complex **22** presumably results from proton exchange from an amido centre to a phosphorus centre accompanied by metallation of the remaining NH protons [29]. It is interesting to note that phosphorous acid, $HPO(OH)_2$, is produced by a similar route, i.e. hydrolysis of PCl_3 [30]. A low-temperature single-crystal X-ray diffraction study (Fig. 6, Table 5) showed complex **22** has an ion-contacted dimeric structure with two $[HP(NR)_3]^{2-}$ anions sandwiching four lithium cations.

Each of the phosphorus centers has a distorted tetrahedral geometry, being coordinated to three imido nitrogen atoms and one hydrogen atom. The P–H proton could not be unequivocally located from the electron difference map, but its presence could be discerned from the ^{1}H- and ^{31}P-NMR spectra and from solution infrared spectroscopy. Hence, the ^{1}H spectra in $[D_6]$-benzene, in addition to confirming the presence of 2-methoxyanilido ligands, show a doublet at $\delta = 9.07$ with a coupling constant of 436 Hz, consistent

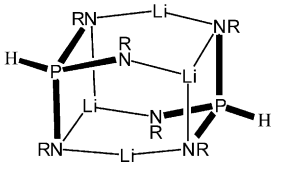

Fig. 6. Line drawing of the structure $[Li_2P(H)\{N(2\text{-}OMe)C_6H_4\}_3]_2$ (**22**).

Table 5
Selected structural data for the lithium salt of imidophosphite dianion

$[HP(NR)_3]^{2-}$	$[Li_2P(H)\{N(2\text{-}OMe)C_6H_4\}_3]_2$ (**22**)
Av. P···N (Å)	1.62
Av. N–P–N (°)	108.8
Li···N (Å)	1.97–2.34
Av. P–N–C (°)	124.6
Reference	[29]

with the $^{1}J_{PH}$ coupling frequencies observed in related systems [31]. The corresponding doublet can be observed in the ^{31}P-NMR spectra at $\delta = 0.28$. This bond can also be observed by IR spectroscopy with a band at 2266 cm^{-1} in THF solution being attributed to the P–H stretching frequency. The phosphorus atoms are bound ca. equally to each imido nitrogen atom {with P–N distances ranging from 1.613(2) to 1.630(2) Å}. The shorter bond distances in **22** compared with those in the related imido analogue of the orthophosphate anion, $[P(NR)_4]^{3-}$ (**21**) {1.645(4) Å} [24] is perhaps due to the enhanced double bond character in **22** where formally, one P=N bond and two P–N bonds form a resonance hybrid, whereas in **21** the ratio is one P=N bond to three P–N bonds.

Within the core of **22** there are two distinct lithium environments. In one domain the lithium centre is complexed by one imido nitrogen centre from each $[HP(NR)_3]^{2-}$ unit and is additionally complexed by two methoxy sidearms of the corresponding methoxyanilido groups. The second lithium environment has the lithium centre complexed by two imido nitrogen atoms from one $[HP(NR)_3]^{2-}$ unit but by only one imido centre from the other $[HP(NR)_3]^{2-}$ unit. The methoxy sidearm of the latter unit completes the distorted tetrahedral geometries about these lithium centers.

It is interesting to note that when **22** is crystallised from THF, a lithium is abstracted from the core and an ion-separated complex, $[Li(THF)_4]^{+}[Li_3\{HP(NR)_3\}_2]^{-}$ is produced. Differences are also observed in the NMR spectra of the compound when it is dissolved in polar and non-polar solvents. Hence, in non-polar solvent a doublet is observed in the ^{31}P-NMR spectra at $\delta = 0.3$ ($^{1}J_{PH} = 436$ Hz) whereas in polar solvent the signal and coupling constant change appreciably ($\delta = 36.9$, $^{1}J_{PH} = 406$ Hz). This may be interpreted as evidence that the two forms observed in the solid state also exist in the appropriate solvent and there is little evidence for an equilibrium between the two. Further studies are required to make this a definitive statement.

3.2.3. Tris(imido) arsenate trianions

Lithium salts of tris(imido) arsenate anions are produced by the reaction of three equivalents of RNH_2 with $AsCl_3$ in THF–NEt_3 followed by metallation with three equivalents of ^{n}BuLi. These complexes form ion-contacted dimers in the solid state whereby two $As(NR)_3]^{3-}$ trianions sandwich six lithium cations in irregular 14 membered core configurations whose degrees of distortion are dictated by the differing ways in which the lithium cations are solvated.

Wright et al. describe the synthesis and structure of the first example of a tris(imido) arsenate trianion, $[Li_3As(N^{t}Bu)_3]_2$ (**23**), from the metallation of ^{t}BuN(H)Li with $As(NMe_2)_3$ in the presence of ^{t}BuNH$_2$ (3:1:3 equivalents) in hexane [32]. The reaction proceeds

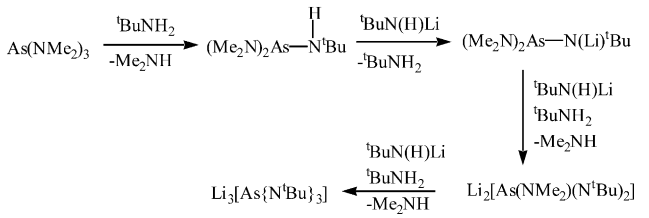

Scheme 4.

by transamination of the amine followed by base abstraction of the remaining proton as is shown in Scheme 4. It is not apparent why the more direct route which has been successfully employed in the preparation of tris(imido) antimony trianions, i.e. the reaction of $As(NMe_2)_3$, is unsuccessful in this case.

However, the X-ray structural analysis of **23** serves only to confirm the assignment of the compound since it is heavily disordered, negating the calculation of precise bond dimensions. An alternative synthesis of tris(imido)arsenate trianions $[Li_3As(NR)_3]_2$ {R = (2-OMe)C_6H_4 **24**; R = CH_2Ph, **25**}, is observed from the reactions of $AsCl_3$ with three equivalents of RNH_2 in THF–NEt_3 followed by metallation with three equivalents of ^{n}BuLi. Low-temperature X-ray structure experiments on complexes **24** and **25** reveal that both complexes have ion-contacted dimeric structures whereby two $[As(NR)_3]^{3-}$ anions are linked together by six lithium cations in 14 membered $As_2N_6Li_6$ cages (see Fig. 7). This is similar to the cage motif observed for **23** [32] but the absence of significant disorder in **24** and **25** allows access to detailed geometrical data.

There are considerable variations from regular D_{3d} symmetry in the As–Li–N networks that form the cores of these polyhedral cages. Whereas the core of complex **25** is probably best viewed as a single $As_2Li_6N_6$ cage, complex **24** is significantly distorted and perhaps should be represented as an $As_2Li_4N_6$ rectangular parallelopiped with two N–N vectors each being capped by additional 'pendant' lithium atoms (see Fig. 7). The ready flexibility of the $[As(NR)_3]^{3-}$ trianion unit in accommodating these distortions is seen in the fact that complex **24** crystallises in the same space group {$P2(1)/c$} with two different unit cells. In both crystalline forms of **24**, one molecule of THF coordinates to each monomer unit. An additional molecule of THF is

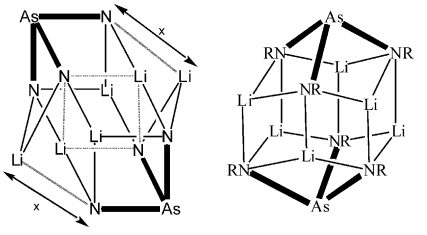

Fig. 7. Line drawing of the structures of $[Li_3As(NR)_3]_2$ {R = (2-OMe)C_6H_4, **24**; R = CH_2Ph, **25**}.

Table 6
Selected structural data for the lithium salts of tris(imido)arsenate trianions. a) A third reported tris(imido) arsenate trianion, $[As(N^tBu)_3]^{3-}$, [32] is too disordered to reveal precise molecular dimensions. b) This molecule was found to crystallise in two forms. The first figure given is for the form that contains two molecules of THF and the second figure are for the form that contains a single molecule of THF

$[As(NR)_3]^{3-}$ [a]	R=(2-OMe)C_6H_4 [b] (**24**·THF)	R = (2-OMe)C_6H_4 [b] (**24**·2THF)	R = CH_2Ph (**25**)
Av. As···N (Å)	1.87	1.87	1.88
Av. N–As–N (°)	93.8	94.2	99.4
Li···N range (Å)	1.96–2.23	1.96–2.16	2.02–2.11
Av. As–N–C (°)	119.4	118.4	110.3
Reference	[33]	[33]	[33]

included in one of the lattices. Furthermore, the differences between the two forms of **24** are evident not only from the different solvation of the crystal lattice but from subtle differences in the bonding within the structures. The principal difference is that the lithium atoms described as 'pendant' to the central core of **24** adopt different positions relative to the core. Hence, the distance (labelled x in Fig. 7) between the pendant Li cation and the imido N on the other $[As(NR)_3]^{3-}$ anion is 2.588(4) Å in **24**·THF and 2.767(6) Å in **24**·2THF. There are also some subtle differences in the binding within each of the cores in the two different forms of **24** and these are outlined in the structure descriptions below (Table 6).

Within each of the structures, the arsenic centers are coordinated by three imido groups in highly distorted trigonal pyramidal geometries. The ca. 5° difference in the mean N–As–N angles between the structures of **24** and **25** highlights the flexibility of the $As(NR)_3$ units in accommodating the distortions of the core structures described above. However, whilst similar phosphorus complexes have distorted tetrahedral geometries about the pnictide centre {e.g. av. N–P–N 108.8° in **22**; [29] av. N–P–N 104.2° in **21** [34]}, this is far less pronounced for the imido arsenic anions reported here. This trend continues for the corresponding imido antimony anions which are described in Section 3.2.4 (in $[Li_3Sb(NR)_3]_2$ av. N–Sb–N 91.8° for R = ^{t}Bu, 90.8° for R = 2,4-dimethoxyphenyl, 93.4° for R = cyclohexyl, 94.5° for R = CH_2CH_2Ph), [35,36] and probably reflects increasing p orbital usage in the imido pnictide bond as the group is descended.

There are considerable variations in the Li–N distances within the complexes. This is probably the result of lithium solvation of **25** being composed of solely Li–N and Li–O(THF) interactions whereas in the structures of **24**, there is competition for binding to Li from not only imido N centers and THF ligands but additionally from the methoxy sidearms of the anisyl groups. This competition results in the lithium atoms being less tightly held in the 14 membered core of **24** compared with **25** and probably exacerbates the distortion in the core of **24**.

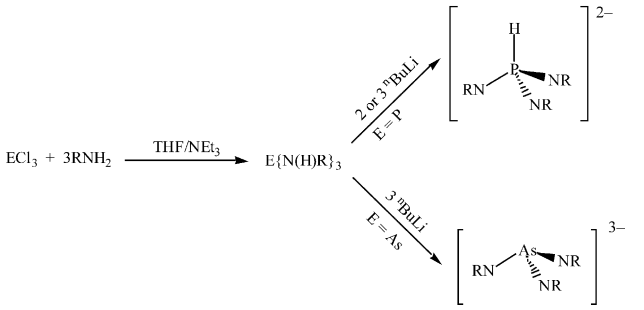

Scheme 5.

The dimensions of the $[As(NR)_3]^{3-}$ moiety may provide an insight into the nature of this trianion. It is interesting to note that, whereas comparable imido phosphorus complexes possess P–N bond lengths that are intermediate in length between commonly accepted values for single and double bonds, [24,29] the corresponding As–N distances observed in this work are very much in the realm for the commonly accepted values for single bonds.

Notably, in the phosphorus reaction, metallation results in a proton shift from an amide {N(H)R} centre to the phosphorus centre, giving the observed $[Li_2HP(NR)_3]_2$ fragment. However, for the corresponding arsenic reactions that produce complexes **24** and **25**, only $[Li_3As(NR)_3]_2$ fragments are observed (highlighted in Scheme 5).

3.2.4. Tris(imido) antimony trianions

The use of tris(dimethylamido) pnictide compounds as potent bases towards primary amines and alkali metal amides (and indeed phosphides) has previously been alluded to in Section 3.2.3 in the preparation of tris(imido) arsenate cages. However, far more intensive investigations have been made using tris(dimethylamido) antimony as a base. These wide ranging studies have highlighted the breadth of different complexes that can be accessed by simple control of stoichiometry in the reactants. Since this review is concerned with only imido analogues of oxoanions and not imido p-block complexes in general, only tris(imido) antimony trianions (the analogue of the antimonate trianion) will be discussed. The interested reader is directed towards

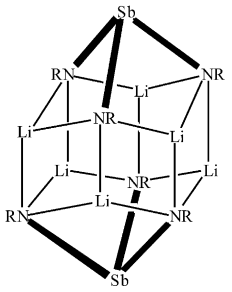

Fig. 8. Line drawing of the core cage of the structures of $[Li_3Sb(NR)_3]_2$ (**26**–**29**).

Table 7
Selected structural data for the lithium salts of tris(imido) antimony trianions

$[Sb(NR)_3]^{3-}$	R=CH_2CH_2-Ph (**26**)	R = $(OMe)_2$-C_6H_3 (**27**)	R=Cy (**28**)	R = ^{t}Bu (**29**)
Av. Sb···N (Å)	2.06	2.05	2.07	2.07
Av. N–Sb–N (°)	94.5	90.8	93.4	91.8
Li···N range (Å)	1.99–2.16	2.01–2.33	1.99–2.17	2.03–2.08
Av. Sb–N–C (°)	111.4	119.3	114.2	118.4
Reference	[36]	[35]	[35]	[35]

recent reviews in this journal for a more in depth discussion of the synthetic applications of dimethylamido reagents and the applications of the products [37,38].

Reaction of the lithium salts of primary amines, $[Li\{N(H)R\}]_n$ with $Sb(NMe_2)_3$ has been shown to produce tris(imido) antimony trianions, $Li_3[Sb(NR)_3]$ for a range of organic groups (R = CH_2CH_2Ph, **26**; $(OMe)_2C_6H_3$, **27**; Cy, **28**; ^{t}Bu, **29**). X-ray crystallographic studies (Fig. 8, Table 7) have shown that all form dimeric structures similar to those of the related tris(imido) arsenate cages detailed in Section 3.2.3.

The influence of Lewis base solvation upon the distortions of the central $Sb_2N_6Li_6$ core is apparent from a close analysis of the structures. In particular, intramolecular donation in complex **27** provides competition for Li solvation between the imido N centers and the O methoxy side-arm donors such that the core becomes extremely distorted {in a similar manner to the tris(imido) arsenic trianions **24** and **25** discussed in Section 3.2.3}. It has been argued persuasively that the variations in the core structures demonstrate that the Group 15 trianion units are the dominant factor in determining the structural arrangement and not the Li···N contacts which feature prominently in the complexes. This view is reinforced by observations of the reactivity of the tris(imido) antimony complexes where the $[Sb(NR)_3]^{3-}$ unit remains intact. Hence, reaction between **27** and Cp_2Pb produces the cage complex $[Pb_3\{Sb(NR)_3\}_2]$ (**30**) where two intact tris(imido) antimony units symmetrically complex three lead centers. A further example of the robust nature of these trianions is the reaction between **28** and KO^{t}Bu (1:3 equivalents) whereby a trimeric K_3O_3 unit inserts into the two $Li_3Sb(NR)_3$ monomers to form $[K_3(O^t\text{-}Bu)_3\{Li_3Sb(NCy)_3\}_2]$ (**31**). The reaction to form this heterotrimetallic cocomplex is presumably driven by the strong Li–O bonds that are formed. Selected bond dimensions for the tris(imido) antimony units of **30** and **31** are given in Table 8.

Table 8
Selected structural data for the non-lithium salts and adducts of tris(imido) antimony trianions

$[Sb(NR)_3]^{3-}$	$[Pb_3\{Sb(NR)_3\}_2]$ (**30**)	$[K_3(O^tBu)_3\{Li_3Sb(NCy)_3\}_2]$ (**31**)
Av. Sb···N (Å)	2.04	2.06
Av. N–Sb–N (°)	85.7	91.3
Li···N range (Å)	–	1.99–2.02
Av. Sb–N–C (°)	119.8	116.0
Reference	[39]	[40]

These data serve to show that the tris(imido) antimony unit is readily flexible in accommodating a new range of coordination geometries (note in particular the compressed N–Sn–N angle in **30** compared with **27**) and highlight the integrity of the $[Sb(NR)_3]^{3-}$ unit as a ligand.

3.3. Group 16

With such a rich oxoanion chemistry, it would be expected that sulfur would possess a correspondingly wide range of imido compounds. Indeed, the S–N link is commonplace and as such it is no surprise to discover a large number of imido sulfur complexes. However, the less stable Se–N and Te–N units also figure prominently. The imido analogues of the sulfate anion, $[SO_4]^{2-}$, the sulfite anion, $[SO_3]^{2-}$, the selenite anion, $[SeO_3]^{2-}$ and the tellurite anion, $[TeO_3]^{2-}$ have been characterised and will be discussed below. A recent review in this journal by Fleisher and Stalke has reviewed the reactivity and coordination behaviour of the sulfur polyimido anions $[S(NR)_n]^{m-}$ [7]. The results of these studies will be summarised here and the reader will be directed to this review and to the primary reports at the appropriate junctures.

3.3.1. Tris(imido) chalcogenite dianions

The first report of an imido analogue of the tellurite anion came as far back as 1967 when Schmitz-DuMont and Ross reported the reaction of diphenyl telluride with potassium amide in liquid ammonia (7:10:2 equivalents) which, upon warming to 20 °C, produces colorless and highly explosive crystals of $K_2[Te(NH)_3]$ (**32**), formally the parent imido analogue of the tellurite anion [41]. Interestingly, neither the sulfur nor selenium reactions yield the equivalent product, with SPh_2 reacting under similar conditions to form PhSK and aniline, and remarkably $SePh_2$ reacts to form selenaanthracene (**33**) (Fig. 9).

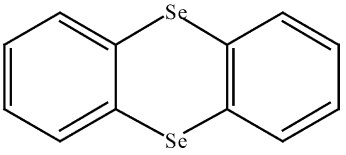

Fig. 9. Selenaanthracene (**33**).

The electronegativity of the chalcogenide is thought to be instrumental in determining the product of the reaction. Ammonolysis, with concomitant formation of benzene, is only observed if the electronegativity is lower than that of the phenyl *ipso*-carbon center.

More recent work has allowed significant advances in Te–N chemistry, fortunately without the undesirable explosive properties! A route has been developed which allows access to stable imido salts not only of tellurium but also of selenium and sulfur. Nucleophilic addition of the lithium salts of primary amines to diimidochalcogenide reagents leads to elimination of amine and produces the imido analogues of the chalcogenite dianion, $[E(NR)_3]^{2-}$ (see Scheme 6). Due to the polarity of the E–N bond ($E^{\partial+}\cdots N^{\partial-}$), the nucleophile always adds to the chalcogenide atom.

This reaction was first utilised by Chivers et al. in 1995 to produce $[Li_2Te(N^tBu)_3]_2$ (**34**), the imido analogue of the tellurite dianion [8]. More recent studies, firstly by the group of Stalke and secondly by Chivers et al., have produced $[Li_2E(N^tBu)_3]_2$ (E = S, **35**, E = Se, **36**), the imido analogues of the sulfite and selenite dianions, respectively, [9,42].

X-ray crystal structures were reported for all of these unsolvated dianions (for R = ^{t}Bu). A commonly recurring structural type is observed in $[E(NR)_3]^{2-}$ (E = S, Se, Te) which form hexagonal prismatic $Li_4E_2(NR)_6$ cores of molecular C_{2h} symmetry (Fig. 10, Table 9), that encompass cages which readily accommodate strong Li–N contacts in arrangements similar to those that are

$$E(NR)_2 + 2LiN(H)R \xrightarrow{E=S,\,Se,\,Te} Li_2E(NR)_3 + RNH_2$$

Scheme 6.

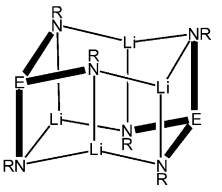

Fig. 10. Line drawing of the structures of $[Li_2E(NR)_3]_2$ (R = ^{t}Bu, E = S, **35**; R = ^{t}Bu, E = Se, **36**; R = ^{t}Bu, E = Te, **34**).

Table 9
Selected structural data for the lithium salts of tris(imido) chalcogenite dianions

$[E(NR)_3]^{2-}$	$[S(N^tBu)_3]^{2-}$ (**35**)	$[Se(N^tBu)_3]^{2-}$ (**36**)	$[Te(N^tBu)_3]^{2-}$ (**34**)
Av. E···N (Å)	1.65	1.80	1.97
Av. N–E–N (°)	102.1	98.8	94.5
Li···N range (Å)	1.92–2.10	1.99–2.12	1.99–2.15
Av. E–N–C (°)	116.3	116.9	117.7
Reference	[42]	[9]	[43]

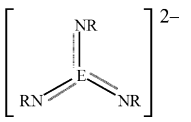

Fig. 11. One of the resonance hybrid structures for $[E(NR)_3]^{2-}$.

well known in lithium amide chemistry [10,11]. A diagram of the cages is shown in Fig. 10 and a summary of the dimensions of these various cages is given in Table 9.

The chalcogen–nitrogen bond lengths in all three dianions are consistent with a degree of multiple bonding that would be expected from the resonance hybrid (shown in Fig. 11) giving a formal bond order of 1.33 for each bond.

The N–E–N bond angles decrease as the group is descended which is consistent with the lone pair on the chalcogen becoming more core like and inert. Hence, there is an increasing predominance of p orbitals in bonding for the heavier chalcogens. Solvation of the core of the imidosulfite complex by THF has a significant effect on the core structure [42]. Only three lithium atoms bind the two $S(N^tBu)_3$ units together. The fourth Li atom bridges two imido units of one the imidosulfite moieties and is further coordinated by a THF molecule. This reaction probably relieves steric crowding and electrostatic repulsions in the relatively compact 12 atom core (Fig. 12).

All three imidochalcogenite complexes show a solitary signal for the ^{t}Bu groups in the ^{1}H-NMR spectra (two resonances due to ^{t}Bu groups would be expected in ratio

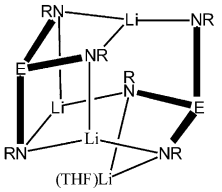

Fig. 12. Line drawing of the structure of $[Li_2S(NR)_3]_2 \cdot THF$ (**35**·THF).

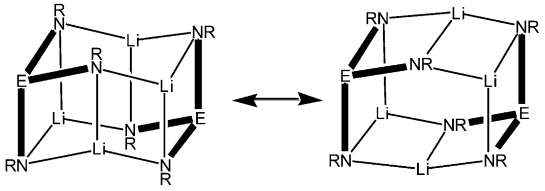

Fig. 13. Fluxional deformation of the imidochalcogenite core.

2:1 from symmetry considerations). This holds true for complexes **34** and **36** over the temperature range 185–298 K. This fluxional behaviour is thought to be a result of deformation of the Li···N core that can readily distort and reform in an apparently low energy process [43] (Fig. 13).

The reactivity of all three complexes has been investigated, particularly the sulfur and tellurium complexes. The reactivity can be broadly classified as follows.

3.3.1.1. Formation of adducts with alkali metal salts. Both complexes **35** and **36** readily bind alkali metal salts to form mixed alkali metal/mixed anion species. The products are either monomeric {E = S, MX = LiBr (**37**), LiI (**38**); [7,44] E = Te, MX = LiCl (**39**), LiBr (**40**), LiI (**41**), [45]}, dimeric {E = S, MX = NaO^{t}Bu (**42**), KO^{t}Bu (**43**); [46] E = S, $M_2X = Li_2S$ (**44**), Na_2S (**45**) [7]}, or polymeric {E = S, MX = LiN_3 (**46**) [47]} depending on the nature of the anion employed. One of the driving forces of these reactions is thought to be the coordination of a third alkali metal ion to the tris(imido) chalcogenite dianion which allows full delocalisation of the negative charges over the ligand backbone. The tris(imido) chalcogenite units themselves are largely unaffected structurally by the adduct formation (Tables 10 and 11), but the data do reflect the flexibility of the anions.

3.3.1.2. Oxidation to form radicals. Complexes **35** and **36** are oxidised by even trace amounts of oxygen (complex **35** may also be oxidised by chlorine and bromine) to form stable radical anions, $[Li_3\{E(N^tBu)_3\}_2]$ (E = S, **47**; E = Se, **48**), where one Li^+ cation and one electron have been removed from the parent species [44,48]. These species have been extensively investigated by ESR spectroscopy. The structures of the products are thought to be a pyramidal tris(imido)chalcogenite radical anion linked through three lithium centers to a pyramidal tris(imido)chalcogenite dianion. Complex **47** is stable for several weeks when oxidised with oxygen (it is far less stable upon halogen oxidation), whereas complex **48** is only stable for a matter of hours. The final product of oxidation of **47** with oxygen is thought to be $[(RN)_3SO]^{2-}$, whereas use of halogens provides a straightforward synthesis of sulfur triimides.

3.3.1.3. Transmetallation reactions. Transmetallation reactions of both the sulfur complex **35** and the tellurium complex **34** have been extensively investigated. Complex **34** reacts with two molar equivalents of $PhPCl_2$ to produce the unusual spirocyclic complex $Ph(N^tBu)P(\mu\text{-}N^tBu)_2Te(\mu\text{-}N^tBu)_2P(N^tBu)Ph$ (**49**) by

Table 10
Selected structural data for the monomeric salt adducts of tris(imido) chalcogenite dianions

$[E(NR)_3]^{2-}$	$[(THF)_3Li_3(\mu_3\text{-Br})\{S(N^tBu)_3\}]$ (**37**)	$[(THF)_3Li_3(\mu_3\text{-I})\{S(N^tBu)_3\}]$ (**38**)	$[(THF)_3Li_3(\mu_3\text{-I})\{Te(N^tBu)_3\}]$ (**41**)
Av. E···N (Å)	1.67	1.66	1.98
Av. N–E–N (°)	100.4	100.4	92.0
Av. E–N–C (°)	118.0	117.1	Data unavailable
Reference	[44]	[44]	[45]

Table 11
Selected structural data for the dimeric and polymeric salt adducts of tris(imido) sulfite dianions [a]

$[E(NR)_3]^{2-}$	$[(THF)_2Li_4Na_2(O^tBu)_2\ \{S(N^tBu)_3\}_2]$ (**42**)	$[(THF)_2Li_4K_2(O^tBu)_2\ \{S(N^tBu)_3\}_2]$ (**43**)	$[(THF)_2Li_3(\mu_4\text{-}N_3)\ \{S(N^tBu)_3\}]_\infty$ (**46**)
Av. E···N (Å)	1.65	1.64	1.64
Av. N–E–N (°)	102.0	102.2	100.6
Av. E–N–C (°)	117.0	116.9	119.2
Reference	[46]	[46]	[47]

[a] Complexes $[(THF)_4Li_6S\{S(N^tBu)_3\}_2]$ (**44**) and $[(THF)_4Li_4 \cdot Na_2S\{S(N^tBu)_3\}_2]$ (**45**) were mentioned in reference [7] but the data were not reported.

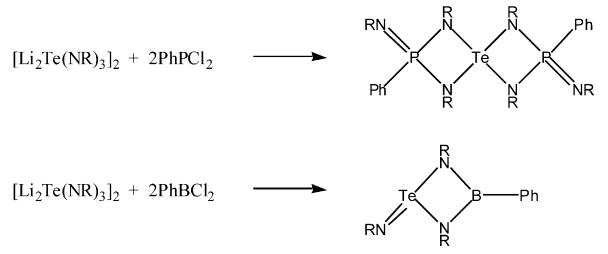

Scheme 7.

transfer of an imido group from the tellurium centre to the phosphorus centre with corresponding oxidation of the phosphorus centre. A similar reaction, that of **34** with two molar equivalents of $PhBCl_2$ produces $PhB(\mu\text{-}N^tBu)_2Te(N^tBu)$ (**50**) in what appears to be a straightforward salt elimination reaction. However, the discovery of cyclic tellurium(II) imides $(^tBuNTe)_3$ in the reaction mixture serves to highlight the complex nature of the reaction mixture (Scheme 7).

Similarly, transmetallation reactions of **34** with MCl_3 (M = Sb, Bi) produce the heterotrimetallic species $Li\{M[Te(N^tBu)_3]_2\}$ (M = Sb, **51**; M = Bi, **52**) [49]. Data from the X-ray structures of **51** and **52**, where the tris(imido) tellurite dianion remains intact are given in Scheme 8 and Table 12.

Interestingly, attempts at 'conventional' transmetallation reactions of complex **35** with Group 14 metal(II) halides result in the decomposition of the $[S(N^tBu)_3]^{2-}$ dianion and the formation of cubane type structures of *tert*-butylimido metal species. However, transmetallation of **35** with main group metal amides, $M\{N(SiMe_3)_2\}_2$ (M = Sn, Ca, Ba), furnishes hexamethyldisilazido lithium and the corresponding mixed metal complexes of the tris(imido) sulfite dianion, $[(THF)_2Ba_2Li\{N(SiMe_3)_2\}\{S(N^tBu)_3\}_2]$ (**53**), $[(THF)_2CaLi_2\{S(N^tBu)_3\}_2]$ (**54**) and $[(THF)SnLi\{N(SiMe_3)_2\}\{S(N^tBu)_3\}]$ (**55**) [50] (Scheme 9, Table 13).

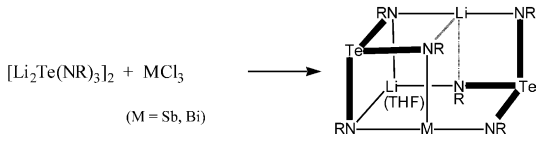

Scheme 8.

Table 12
Selected structural data for the heterobimetallic salts of tris(imido) tellurite dianions

$[Te(NR)_3]^{2-}$	$Li\{Sb[Te(N^tBu)_3]_2\}$ (**51**)	$Li\{Bi[Te(N^tBu)_3]_2\}$ (**52**)
Av. E···N (Å)	1.97	1.97
Av. N–E–N (°)	92.7	93.1
Av. E–N–C (°)	118.3	118.4
Reference	[49]	[49]

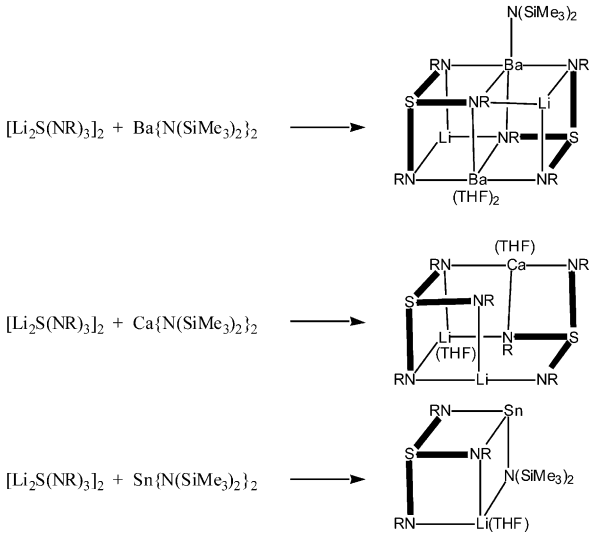

Scheme 9.

Taken as a whole, the tris(imido) sulfite dianions demonstrate a remarkable electronic versatility in their coordination behaviour. Two of the three resonance forms (labelled A and C in Fig. 14) have been identified, and it is argued that this electronic flexibility may help explain the unusual high stability of the radical anions that have been observed.

The reactions used to form **51**–**55** and the data in Tables 12 and 13 demonstrate that the tris(imido)chalcogenite dianions are flexible entities as ligands to a range of different metal centers. As with the tris(imido) pnictide anions (Section 3.2) it would be argued that the imidochalcogenite units are dominant over the Li···N contacts in determining the structural arrangement.

3.3.2. *Imidosulfate dianions*

In contrast to the intensive studies into the tris(imido) chalcogenite dianions, the corresponding imido analogues of the chalcogenate ions have been investigated rather less, but are nonetheless exciting. Early reports from Appel and Ross (based on evidence that would not be considered strong by today's standards) revealed that the reaction of *S*,*S*-dimethyl sulfur diimine with KNH_2 in liquid ammonia produces $[K_3(NH)_3SN\cdot NH_3]$ (**56**), formally the tripotassium salt of the hypothetical parent imido–amido analogue of sulfuric acid, $H_2S(NR)_4$ [51,52]. Recently, more rigorous characterisation has revealed the imido analogue of lithium sulfate, $[(THF)_4Li_2S(N^tBu)_4]$ (**57**), synthesised by a similar method used to produce the chalcogenite ions, i.e. nucleophilic addition of lithium amide to a multiple bond (in this case addition to a sulfur triimide) [53] (Scheme 10).

Unlike lithium sulfate, which exists as an infinite solid-state structure, the imido analogue is revealed by an X-ray crystallographic study (Fig. 15, Table 14) to be

Table 13
Selected structural data for the heterobimetallic salts of tris(imido) sulfite dianions

$[S(NR)_3]^{2-}$	$[(THF)_2Ba_2Li\{N(SiMe_3)_2\}\{S(N^tBu)_3\}_2]$ (**53**)	$[(THF)_2CaLi_2\ \{S(N^tBu)_3\}_2]$ (**54**)	$[(THF)SnLi\{N(SiMe_3)_2\}\{S(N^tBu)_3\}]$ (**55**)
Av. E···N (Å)	1.60	1.65	1.66
Av. N–E–N (°)	102.7	108.0	101.0
Av. E–N–C (°)	116.0	117.3	117.6
Reference	[50]	[50]	[50]

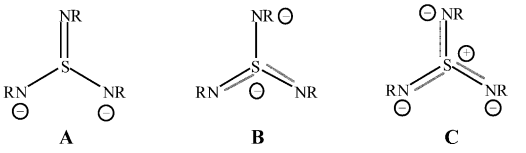

Fig. 14. Three resonance hybrid structures for $[S(NR)_3]^{2-}$.

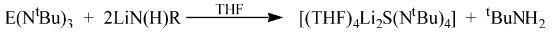

Scheme 10.

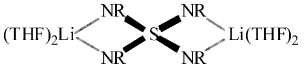

Fig. 15. Line drawing of the structure of $[Li_2S(NR)_4\cdot 2THF]_2$ (**57**).

Table 14
Selected structural data for the lithium salt of the imidosulfate dianion

$[S(NR)_4]^{2-}$	$[S(N^tBu)_4]^{2-}$ (**57**)
Av. S···N (Å)	1.60
Av. N–S–N (°)	94.7 (bridged) and 117.4 (non-bridged)
Li···N range (Å)	1.95–1.97
Av. S–N–C (°)	125.4
Reference	[53]

Table 15
Selected structural data for the non-lithium salt of the imidosulfate dianion

$[S(NR)_4]^{2-}$	$[(THF)_4Ba_2\{N(SiMe_3)_2\}_2S(N^tBu)_4]$ (**58**)
Av. S···N (Å)	1.60
Av. N–S–N (°)	96.3 (bridged) and 116.5 (non-bridged)
Av. S–N–C (°)	125.3
Reference	[54]

a discrete entity with THF solvation preventing further aggregation. Complex **57** adopts a structure similar to the ion-separated monoanion in the isoelectronic imido analogue of the phosphate trianion **21**. Hence, each lithium bridges two imido moieties from a distorted tetrahedral $S(N^tBu)_4$ unit and is additionally ligated by two THF molecules.

In a similar manner to the imidochalcogenite complexes **35** and **36**, complex **57** is readily oxidised by

Group 13	Group 14	Group 15	Group 16
$[B(NR)_3]^{3-}$	$[C(NR)_3]^{2-}$		
	$[Si(NR)_4]^{4-}$	$[HP(NR)_3]^{2-}$	$[SNR)_3]^{2-}$
		$[P(NR)_4]^{3-}$	$[S(NR)_4]^{2-}$
		$[As(NR)_3]^{3-}$	$[Se(NR)_3]^{2-}$
		$[Sb(NR)_3]^{3-}$	$[Te(NR)_3]^{2-}$

Fig. 16. Imido analogues of p-block oxoanions.

oxygen to give an intensely coloured solution, although the product(s) have not been unequivocally characterised to date. Similarly, attempts to isolate the imido analogue of sulfuric acid, $H_2S(N^tBu)_4$, have yet to bear fruit, although in situ preparation of $H_2S(N^tBu)_4$, followed by deprotonation with $[(THF)_2Ba\{N(SiMe_3)_2\}_2]$ yields $[(THF)_4Ba_2\{N(SiMe_3)_2\}_2S(N^tBu)_4]$ (**58**). The structural parameters for the lithium and barium salts (see Tables 14 and 15) indicate that the imidosulfate dianion adopts a very similar geometry in the structures despite the different natures of the counterions.

4. Summary and outlook

Perhaps the best way to sum up the advances that have been made in preparing imido analogues of p-block oxoanions is to present a figure (see Fig. 16) that bears comparison to that of the p-block oxoanions that are shown in Fig. 1.

One of the most notable observations from a comparison of Figs. 1 and 16 is the absence of imido analogues of p block oxoanions with a halogen as the central element. This is probably related to the synthetic routes available towards such complexes. For example, there are few suitable starting materials for the application of the synthetic protocols highlighted in Section 2. In addition, there is also the potential for alternative reaction pathways, such as the formation of metal halide salts upon reaction with organometallic reagents. The development of reaction pathways towards imido haloanions is a great synthetic challenge in this area of chemistry.

A feature of many of the complexes that have been described in this review is that they have been prepared as lithium salts. In many ways the lithium acts as a

'magic glue' in binding together the anions to form complexes that are readily amenable to standard laboratory characterisation techniques. X-ray crystallography experiments have shown that many of these p-block imido anions aggregate as intricate cage structures that are readily distorted by both inter- and intramolecular Lewis base solvation. One trend that is apparent from the dimensions of these cage structures is the decrease in N–E–N angle as the group is descended. This probably reflects increasing p orbital involvement in bonding among the heavier p-block elements. In addition, the imido centre in all of the p-block element anions described herein possesses a bent N atom which would be considered formally sp^2 hybridised, and the ligand will be formally a $4e^-$ ($\sigma+\pi$) donor system. The extent of π-overlap is a subject of some debate and would undoubtedly benefit from detailed theoretical investigations.

These imido anions have been found to act both as ligands to other metals and as imido transfer reagents to other species. In the former mode, the anions display a ready flexibility in coordinating to a range of metals. However, further examples of the coordination behaviour of a wide range of p-block imido anions are required before the potential of such ligand systems can be fully explored. It is noteworthy that related complexes have found application as polyolefin catalysts [55]. In addition, many of the anions described possess stereochemically active lone pairs at the p-block element centre as well as lone pairs on the nitrogen atoms. They should, therefore, coordinate both hard and soft Lewis acids, although no experimental reports of this behaviour have appeared in the literature to date.

Acknowledgements

We would like to acknowledge the generous funding of The Royal Society (Research Fellowship for C.A.R.), the EPSRC (C.A.R., M.C.C., G.M.A.) and The University of Bristol (C.A.R., A.P.L.).

References

[1] D.E. Wigley, Prog. Inorg. Chem. 42 (1994) 239.
[2] J.K. Brask, T. Chivers, G. Schatte, Chem. Commun., (2000) 1805.
[3] J.C. Jeffery, A.P. Leedham, C.A. Russell, Polyhedron, in press.
[4] N.N. Greenwood, A. Earnshaw, Chemistry of the Elements, Oxford, 1997.
[5] N.N. Greenwood and A. Earnshaw, Chemistry of the Elements, Oxford, 1997.
[6] D. Brauer, H. Bürger, G.R. Lienwald, J. Organomet. Chem. 308 (1986) 119.
[7] R. Fleischer, D. Stalke, Coord. Chem. Rev. 176 (1998) 431.
[8] (a) T. Chivers, X. Gao, M. Parvez, Angew. Chem., 107 (1995) 2756;
(b) Angew. Chem. Int. Ed. Engl. 34 (1995) 2459.
[9] T. Chivers, M. Parvez, G. Schatte, Inorg. Chem. 35 (1995) 4094.
[10] R.E. Mulvey, Chem. Soc. Rev. 20 (1991) 167.
[11] K. Gregory, R. Snaith, P.V.R. Schleyer, Adv. Inorg. Chem. 37 (1991) 47.
[12] P.J. Bailey, S. Pace, Coord. Chem. Rev. 214 (2001) 91.
[13] N.J. Bremer, A.B. Cutcliffe, M.F. Farona, W.G. Kofron, J. Chem. Soc. A (1971), 3264.
[14] P.J. Bailey, A.J. Blake, M. Kryszczuk, S. Parsons, D. Reed, J. Chem. Soc. Chem. Commun. (1995) 1647.
[15] S. Patai, in: S. Patai (Ed.), The Chemistry of the Carbon–Nitrogen Double Bond, Interscience, 1970.
[16] T. Chivers, M. Parvez, G. Schatte, J. Organomet. Chem. 550 (1998) 213.
[17] M.B. Dinger, W. Henderson, J. Chem. Soc. Chem. Commun. (1996) 211.
[18] M.B. Dinger, W. Henderson, B.K. Nicholson, J. Organomet. Chem. 556 (1996) 75.
[19] P.J. Bailey, L.A. Mitchell, P.R. Raithby, M.-A. Rennie, K. Verhorevoort, D.S. Wright, J. Chem. Soc. Chem. Commun., (1996) 1351.
[20] G. Rodriguez, C.K. Sperry, G.C. Bazan, J. Mol. Cat. A 128 (1998) 5.
[21] J.K. Brask, T. Chivers, M. Parvez, Inorg. Chem. 39 (2000) 2508.
[22] (a) E. Niecke, M. Frost, M. Nieger, V. von der Gönna, A. Ruban, W.W. Schoeller, Angew. Chem. 106 (1994) 2170.;
(b) Angew. Chem. Int. Ed. Engl. 33 (1994) 2111.
[23] R. Detsch, E. Niecke, M. Nieger, W.W. Schoeller, Chem. Ber. 125 (1992) 1119.
[24] (a) P.R. Raithby, C.A. Russell, A. Steiner, D.S. Wright, Angew. Chem. 109 (1997) 670.;
(b) Angew Chem. Int. Ed. Engl. 36 (1997) 649.
[25] N.N. Greenwood, A. Earnshaw, Chemistry of the Elements, Oxford, 1984.
[26] (a) W. Schnick, Angew. Chem. 105 (1993) 846.;
(b) Angew. Chem. Int. Ed. Engl. 32 (1993) 806.
[27] (a) W. Schnick, S. Horstmann, A. Schmidpeter, Angew. Chem. 106 (1994) 818;
(b) Angew. Chem. Int. Ed. Engl. 33 (1994) 785.
[28] D.S. Payne, Topics in Phosphorus Chemistry, New York, 1967.
[29] L.T. Burke, E. Hevia-Freire, R. Holland, J.C. Jeffery, C.A. Russell, A.P. Leedham, A. Steiner, A. Zagorski, J. Chem. Soc. Chem. Commun. (2000) 1769.
[30] J. Novosad, Encyclopedia of Inorganic Chemistry, Chichester, 1994.
[31] A. Schmidpeter, J. Ebeling, H. Stary, C. Weingand, Z. Anorg. Allg. Chem. 394 (1972) 171.
[32] M.A. Beswick, S.J. Kidd, M.A. Paver, P.R. Raithby, A. Steiner, D.S. Wright, Inorg. Chem. Commun. 2 (1999) 612.
[33] L.T. Burke, J.C. Jeffery, A.P. Leedham, C.A. Russell, J. Chem. Soc. Dalton Trans. (2001) 423.
[34] J.C. Jeffrey, A.P. Leedham, C.A. Russell, unpublished results.
[35] M.A. Beswick, N. Choi, C.N. Harmer, A.D. Hopkins, M. McPartlin, M.A. Paver, P.R. Raithby, A. Steiner, M. Tombul, D.S. Wright, Inorg. Chem. 37 (1998) 2177.
[36] (a) A.J. Edwards, M.A. Paver, P.R. Raithby, M.-A. Rennie, C.A. Russell, D.S. Wright, Angew. Chem. (1994) 106 1334;
(b) Angew. Chem. Int. Ed. Engl. (1994) 33 1277.
[37] M.A. Beswick, D.S. Wright, Coord. Chem. Rev. 176 (1998) 373.
[38] A.D. Hopkins, J.A. Wood, D.S. Wright, Coord. Chem. Rev. 216 (1998) 155.
[39] M.A. Beswick, N.L. Cromhout, C.N. Harmer, M.A. Paver, M.-A. Rennie, P.R. Raithby, A. Steiner, D.S. Wright, Inorg. Chem. 36 (1997) 1740.
[40] (a) D. Barr, A.J. Edwards, M.A. Paver, P.R. Raithby, M.-A. Rennie, C.A. Russell, D.S. Wright, Angew. Chem. 107 (1995) 1088.;
(b) Angew. Chem., Int. Ed. Engl. 34 (1995) 1012.

[41] (a) O. Schmitz-DuMont, B. Ross, Angew. Chem. 79 (1967) 1061; (b) Angew. Chem. Int. Ed. Engl. 6 (1967) 1071.
[42] (a) R. Fleischer, S. Freitag, F. Pauer, D. Stalke, Angew. Chem. 108 (1996) 208.; (b) Angew. Chem. Int. Ed. Engl. 35 (1996) 204.
[43] T. Chivers, X. Gao, M. Parvez, Inorg. Chem. 35 (1996) 4336.
[44] R. Fleischer, S. Freitag, D. Stalke, J. Chem. Soc. Dalton Trans. (1998) 193.
[45] T. Chivers, M. Parvez, G. Schatte, Inorg. Chem. 40 (2001) 540.
[46] D. Ilge, D.S. Wright, D. Stalke, Chem. Eur. J. 4 (1998) 2275.
[47] R. Fleischer, D. Stalke, J. Chem. Soc. Chem. Commun. (1998) 343.
[48] J. Brask, T. Chivers, B. McGarvey, G. Schatte, R. Sung, R. Boere, Inorg. Chem. 37 (1998) 4633.
[49] T. Chivers, M. Parvez, G. Schatte, G.P.A. Yap, Inorg. Chem. 38 (1999) 1380.
[50] R. Fleischer, D. Stalke, Organometallics 17 (1998) 832.
[51] R. Appel, W. Ross, Chem. Ber. 102 (1969) 1020.
[52] (a) R. Appel, W. Ross, Angew. Chem. 80 (1968) 561.; (b) Angew. Chem. Int. Ed. Engl. 7 (1968) 546.
[53] (a) R. Fleischer, A. Rothenberger, D. Stalke, Angew. Chem. 109 (1998) 1140.; (b) Angew. Chem. Int. Ed. Engl. 36 (1997) 1105.
[54] R. Fleischer, B. Walfort, A. Gbureck, P. Scholz, W. Kiefer, D. Stalke, Chem. Eur. J. 4 (1998) 2266.
[55] M. Witt, H.W. Roesky, Chem. Rev. 94 (1994) 1163.